

Phase transitions of a simple hexagonal $\text{In}_{0.2}\text{Sn}_{0.8}$ alloy under high pressure

V. F. Degtyareva

Institute of Solid State Physics, Russian Academy of Sciences, Chernogolovka, Moscow district 142432, Russia

O. Degtyareva and W. B. Holzapfel

FB 6 Physik, Universität-Paderborn, 33095 Paderborn, Germany

K. Takemura

National Institute for Research in Inorganic Materials, Tsukuba, Ibaraki 305, Japan

(Received 9 July 1999)

Phase transitions of a Sn-In (20 at. % In) alloy have been studied under pressures up to 30 GPa in diamond anvil cells by energy dispersive and angle dispersive x-ray diffraction. The simple hexagonal low-pressure phase (*hP1*) was found to transform at pressures above 13 GPa to a mixture of two phases: body-centered tetragonal (*tI2*) and close-packed hexagonal (*hP2*). This transformation of the $\text{In}_{0.2}\text{Sn}_{0.8}$ alloy under pressure is considered as a decomposition of the low-pressure phase into a mixture of two phases, whereby the *hP2* phase begins to dominate with the further increase of pressure. Above 23 GPa only the *hP2* phase was observed. The axial ratios for all three phases in $\text{In}_{0.2}\text{Sn}_{0.8}$ and their variations on compression are discussed.

INTRODUCTION

The group IV elements Si and Ge show some common features in their structural changes under pressure with the general trend: *diamond* (*cF8*) \rightarrow *white tin* (*tI4*) \rightarrow *simple hexagonal* (*hP1*) \rightarrow *close-packed structures* (*hP2*, *cF4*).¹⁻⁷ Besides these high-symmetry structures, some intermediate low-symmetry structures have also been observed.^{8,9} Silicon, for instance, transforms from *hP1* to *hP2* through a low-symmetry intermediate phase, Si-VI,² recently determined as *oC16*, space group *Cmca*.¹⁰

The heavier group IV element Sn displays a different structural sequence under pressure with *diamond* (*cF8*) \rightarrow *white tin* (*tI4*) \rightarrow *body-centered tetragonal* (*tI2*) \rightarrow *body-centered cubic* (*cI2*) (Refs. 7 and 11) without *hP1* and related complex structures.

The structural effects of pressure are similar in some cases to the effects of alloying. Sn is known to form *hP1* by alloying with In, Hg, and Cd at normal pressure.¹² In this phase *hP1* the metallic atoms occupy randomly the 1(a) position of *P6/mmm*. Similar phases have been obtained also in more than ten Sn-based alloys by rapid quenching from the melt.¹³ The common feature of the appearance of *hP1* in these alloys is an average valence electron concentration of about 3.8 electron per atom.¹⁴ A recent study on the *hP1* alloy HgSn_9 under pressure¹⁵ revealed the occurrence of a *tI2* phase similar to Sn-III. However, it is not clear so far, whether other *hP1* phases show the same behavior as Si and Ge or as Sn under pressure.

EXPERIMENTAL DETAILS

For these reasons, an alloy of Sn with 20 at. %In was prepared by melting in an evacuated silica tube to obtain another pure *hP1* phase. The measured lattice parameters, $a = 321.7(1)$ pm and $c = 299.8(1)$ pm, were close to previ-

ously reported data.^{16,17} The high pressure experiments used a diamond anvil cell and energy dispersive x-ray diffraction (EDX) with synchrotron radiation in HASYLAB (DESY, Hamburg). Different sets of measurements were performed on $\text{In}_{0.2}\text{Sn}_{0.8}$ with pressure determination by ruby luminescence or gold as x-ray diffraction reference, with or without mineral oil as pressure transmitting medium. Details of the experimental setup are reported in Ref. 18. One series of measurements was performed by angle dispersive x-ray diffraction (ADX) on a M18X diffractometer with MoK_α radiation using an image-plate area detector at NIRIM, Tsukuba. Also this technique has been described previously.¹⁹ In all cases the diffraction spectra were obtained at room temperature. In two series the sample was annealed under pressures of 13–15 GPa at 150–175 °C for 2–3 h to reduce strain effects and eliminate kinetic hindrance.

RESULTS AND DISCUSSION

Two transitions were observed in the $\text{In}_{0.2}\text{Sn}_{0.8}$ alloy on increasing pressure to 30 GPa. The diffraction pattern of the low-pressure *hP1* phase (Fig. 1) persists up to 10 GPa. At higher pressure new diffraction patterns appear as a result of a phase transition. No diffraction peak of *hP1* was observed above 13 GPa, but the diffraction patterns show gradual changes in the relative peak intensities on further increase of pressure up to 23 GPa where only one set of diffraction peaks remains, and the diffraction patterns become much simpler, as shown in Fig. 1. The pattern at 27 GPa can be indexed on the basis of a hexagonal close-packed structure (*hP2*) with lattice parameters $a = 305.0(2)$ pm, $c = 500.7(3)$ pm. For the intermediate state between *hP1* and *hP2* no simple solution was found when the patterns were treated as a single phase.

A perfect indexing of the diffraction pattern for this intermediate state was obtained however by a two-phase mixture

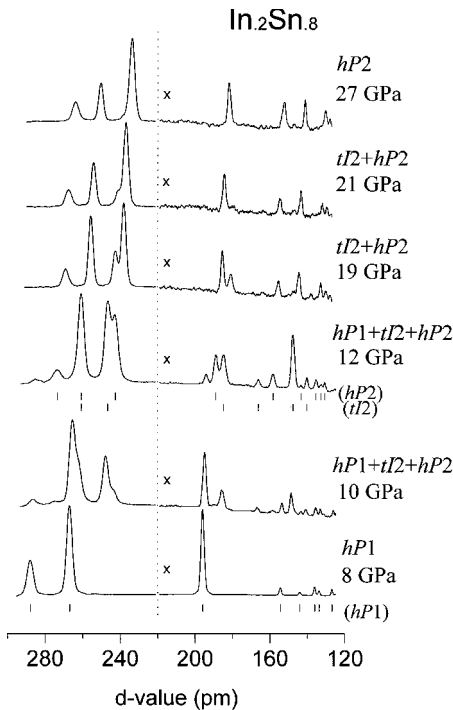


FIG. 1. EDX spectra of $\text{In}_{0.2}\text{Sn}_{0.8}$ taken on increasing pressure. Parts of spectra from 220 to 120 pm are scaled in intensity: spectrum at 8 GPa $\times 1.5$ times, the next spectra $\times 4$ times. The gasket peaks are extracted, parts of spectra with fluorescence peaks are not shown. Bars indicate peak positions for $hP1$ at 8 GPa as well as for $hP2$ and $tI2$ at 12 GPa.

of a close-packed hexagonal ($hP2$) and a body-centered tetragonal ($tI2$). The image plate pattern of the $\text{In}_{0.2}\text{Sn}_{0.8}$ alloy at 13.3 GPa and its integrated profile are shown in Fig. 2. The corresponding indexing of the diffraction peaks is given in detail in Table I, which includes also a comparison of observed and calculated d values and intensities. A random distribution of Sn and In atoms was assumed in the $hP2$ and $tI2$ phases over the sites 2(c) of $P6_3/mmc$ and 2(a) of $I4/mmm$, respectively. Due to the occurrence of texture induced by small deviatoric stress under quasihydrostatic pressures one expects only a qualitative agreement between observed and calculated intensities in this case, nevertheless, the observed agreement supports the present model.

This model of a two-phase mixture explains then the change in diffraction spectra with increasing pressure by a change in the relative amounts of phases in the mixture. Just after the beginning of transition above 10 GPa two new phases are observed with a small amount of the remaining low-pressure phase $hP1$ (Fig. 1). A comparison of the relative intensities indicates that $tI2$ dominates over $hP2$ just after the transition, but finally at pressures above 23 GPa only $hP2$ exists as single phase. It should be noted that the $tI2$ phase has never been observed as single phase (without admixture of $hP2$), neither on compression, decompression or recompression. On decompression the transformations were reversible with small hysteresis: $hP2 \rightarrow tI2 + hP2 \rightarrow hP1$ and below 10 GPa the initial $hP1$ phase is completely recovered.

It should be noted also that both high-pressure phases, $hP2$ and $tI2$, display on the image plate pattern very smooth lines of almost equal quality, whereas the low-pressure phase

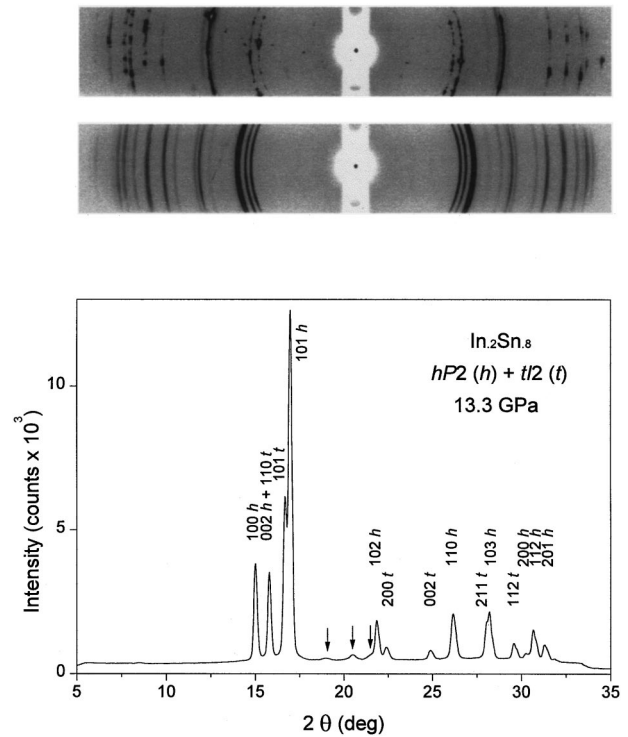


FIG. 2. The image plate patterns of $\text{In}_{0.2}\text{Sn}_{0.8}$: low-pressure simple hexagonal ($hP1$) phase at 6.1 GPa on decompression (above); two-phase mixture of close-packed hexagonal ($hP2$) and body-centered tetragonal ($tI2$) phases at 13.3 GPa (middle). Integrated profile of image plate pattern at 13.3 GPa (below); arrows denote diffraction peaks from gasket material (spring steel with the close-packed hexagonal structure).

$hP1$ has very spotty lines on compression as well as on decompression (Fig. 2). Annealing of the sample under pressure leads to sharper diffraction peaks but does not effect significantly the relative peak intensity, indicating that the relative amounts of the different phases do not change noticeably during the annealing. This behavior implies that the two-phase mixture of the alloy is a stable state in this pressure range and not a metastable state resulting from kinetic hindrances. This means that the direct transition of $hP1$ to this two-phase mixture can be considered as decomposition of the ambient pressure phase ($hP1$) into two phases of different compositions, which is allowed by Gibb's phase rule for a two-component system.

The average atomic volumes for both high-pressure phases are equal within the experimental error in accordance with data at 13.3 GPa shown in Table I, and the volume change at the transition $hP1 \rightarrow tI2 + hP2$ does not exceed 1.5%. With respect to the minor volume discontinuity of the I-II transition and the almost equal volume for both high-pressure phases one can fit one common equation of state^{20,21} to all the data with $K_0 = 50.1(4)$ GPa and $K'_0 = 4.2(7)$ as shown in Fig. 3. These parameter values are close to those for $\text{Hg}_{0.1}\text{Sn}_{0.9}$ (Ref. 15) and also for pure Sn.²²

It is interesting to analyze axial ratios for uniaxial (non-cubic) structures and their variations on compression to understand the factors that stabilize these structures. Figure 4 represents the axial ratio for all three phases of $\text{In}_{0.2}\text{Sn}_{0.8}$ plotted with respect to the atomic volume. The axial ratio of $hP1$ is 0.932(1) at normal pressure, and it varies with pres-

TABLE I. Observed and calculated d spacings and diffraction intensities of $\text{In}_{0.2}\text{Sn}_{0.8}$ at 13.3 GPa for the two-phase mixture of the $hP2$ phase with $a=315.16(5)$ pm, $c=519.67(14)$ pm for space group $P6_3/mmc$, and the $tI2$ phase with $a=367.61(8)$ pm, $c=331.12(7)$ pm for space group $I4/mmm$.

d_{obs} (pm)	I_{obs}	$hP2$			$tI2$		
		(hkl)	d_{calc} (pm)	I_{calc}	(hkl)	d_{calc} (pm)	I_{calc}
272.87	27	100	272.94	23			
259.85	25	002	259.84	27	110	259.94	58
246.08	47				101	246.03	100
241.68	100	101	241.64	100			
188.02	15	102	188.19	16			
183.86	5				200	183.81	22
165.53	4				002	165.55	8
157.47	20	110	157.58	19			
147.22	15				211	147.25	45
146.27	15	103	146.25	23			
139.66	7				112	139.64	19
136.51	2	200	136.47	3			
134.77	12	112	134.74	23			
132.08	7	201	131.99	16			

sure only very slightly, increasing up to 0.934(1) at 13 GPa. The $hP2$ phase displays a slight decrease of c/a from 1.650(1) at 14 GPa to 1.641(1) at 27 GPa. The $tI2$ phase shows a slight increase of c/a upon compression from 0.893(1) at 16 GPa to 0.908(1) at 21 GPa.

The dashed lines in Fig. 4 show special values of c/a for each phase. The ideal value for the $hP2$ phase $c/a = \sqrt{8/3} = 1.633$ corresponds to close packing of spheres. The trend toward this value under pressure can be rationalized as a result of stronger electrostatic repulsion favoring more symmetrical atomic arrangements.

For the $hP1$ phase a special value was given as $(\sqrt{3}/2)^{1/2} = 0.931$ in Ref. 23, considering a balance between two terms of the electrostatic energy connected with sums in real and reciprocal lattice space. The observation of a very minor change of c/a under pressure for the $hP1$ phase of $\text{In}_{0.2}\text{Sn}_{0.8}$ points to a special stability of the $hP1$ phase at this special value.

The axial ratio for the $tI2$ structure can be related to characteristics of the distortion from cubic symmetry. As discussed earlier^{15,24} this distortion is connected with Fermi-sphere–Brillouin-zone fitting and determined by the condition that the reciprocal lattice vector $2\pi/a_t$ should be not larger than the Fermi-sphere radius k_F , i.e., $2\pi/a_t \leq k_F$. According to this model the degree of distortion increases with a decrease in the number of valence electrons n and can be determined by the relation: $c/a \leq (3/4\pi)n$. If $n = 3.8$, as in the case of the $\text{In}_{0.2}\text{Sn}_{0.8}$ alloy, one finds $c/a \leq 0.907$. An increase of c/a toward this value is clearly observed for the $tI2$ phase in the $\text{In}_{0.2}\text{Sn}_{0.8}$ alloy upon compression (see Fig. 4). This trend was previously noticed also for the $tI2$ phase in the $\text{Hg}_{0.1}\text{Sn}_{0.8}$ alloy which has the same value of $n = 3.8$.¹⁵ For $n = 4.0$, as in the case of Sn and InBi, this estimate gives $c/a \leq 0.955$, in agreement with the experimental results.^{11,22,24} If one considers high pressure $tI2$ phase in both alloys, $\text{In}_{0.2}\text{Sn}_{0.8}$ and $\text{Hg}_{0.1}\text{Sn}_{0.9}$, just as a solid

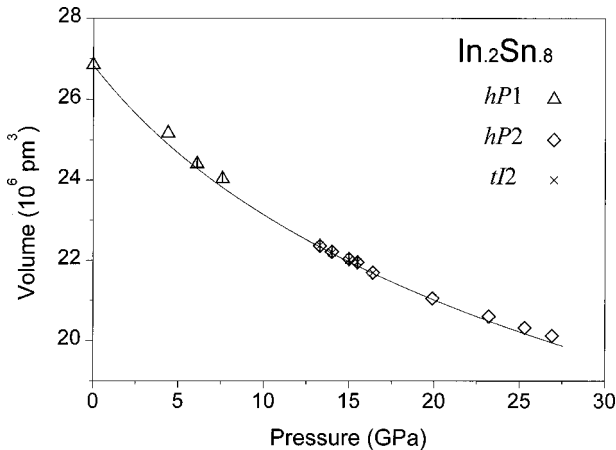


FIG. 3. Pressure dependence of atomic volume of $\text{In}_{0.2}\text{Sn}_{0.8}$ for $hP1$, $hP2$, and $tI2$ phases. The data are fitted by common equation of state (solid line). Open symbols denote EDX data; symbols with sticks denote ADX data.

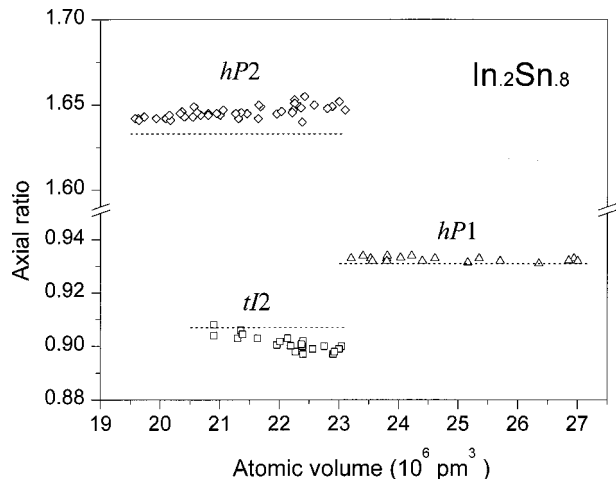


FIG. 4. Axial ratio for $hP1$, $hP2$, and $tI2$ phases vs atomic volume in the $\text{In}_{0.2}\text{Sn}_{0.8}$ alloy. Dashed lines show the special values of the axial ratio for each structure (see text).

solution with respect to the $tI2$ modification of pure Sn, the substitution of Sn by In or Hg reduces the average valence electron concentration, which is then responsible for a decrease of the upper limiting value of c/a .

Since the composition of each of the two phases in the two-phase region can vary also with pressure the axial ratios in Fig. 4 are plotted only as functions of volumes.

From the point of view that both the $\text{In}_{0.2}\text{Sn}_{0.8}$ and $\text{Hg}_{0.1}\text{Sn}_{0.9}$ alloys crystallize at ambient pressure in the same $hP1$ structure, the difference in their behavior under pressure is very essential and should be related to the different amounts of the alloy components. Obviously under pressure, the range of the Sn-based solid solution with $tI2$ structure includes the composition of 10 at. % Hg in the Hg-Sn system, but does not extend to 20 at. % In in the In-Sn system.

A specific feature of the observed transformation in the binary alloy $\text{In}_{0.2}\text{Sn}_{0.8}$ is that a single-phase state ($hP1$) undergoes a transition into a two-phase state ($tI2 + hP2$). This observation implies a decomposition of the $hP1$ phase under pressure into a mixture of the two other phases ($tI2 + hP2$) of different compositions. The $tI2$ phase must be enriched in Sn, whereas the $hP2$ phase must be enriched in In, but finally it extends with increasing pressure toward the Sn-rich side. Above 23 GPa only the $hP2$ phase exists as single phase for this composition.

This decomposition of a low-pressure phase under pressure can be elucidated further by additional high-pressure studies on In-Sn alloys with different concentrations. An example of a direct $hP1 - hP2$ transformation under pressure was found previously in the $\text{Al}_{0.3}\text{Ge}_{0.7}$ alloy.²⁵ On the other hand, a decomposition of zero-pressure phases in a binary alloy system with increasing pressure was previously observed in Zn-Sb and Cd-Sb.^{14,26} The compounds ZnSb and CdSb were shown to decompose into a $hP1$ phase (of about

60 at. % Sb) with segregation of the excess Zn or Cd, respectively.

The present study on the $\text{In}_{0.2}\text{Sn}_{0.8}$ alloy as well as the previous studies on ZnSb and CdSb (Refs. 14 and 26) demonstrate a peculiarity of high-pressure transformations in a two-component system. In comparison with a one-component system the additional degree of freedom (composition) allows for an increase in the number of coexisting phases. Sometimes also decomposition as well as kinetic effects can lead to the formation of amorphous state as is the case of Zn-Sb and Cd-Sb.^{14,26}

CONCLUSION

The present study seems to show the reversible decomposition in an alloy from a low-pressure phase, here $hP1$, into a mixture of two phase, here $tI2$ and $hP2$, whereby the two new phases are distinguished not only by the different structures but also by segregation of initially homogeneous alloy into two phases with different compositions. However, with further increase in pressure the phase compositions vary in such a way that the Sn-rich phase $tI2$ is finally desolved completely in the $hP2$ phase above 23 GPa. These phase transitions and the different stability of $tI2$ and $hP2$ phases for different compositions in the In-Sn alloy system under pressure are certainly of strong theoretical interest for the better understanding of structural stability in group IV elements and their alloys with neighboring elements under pressure.

ACKNOWLEDGMENTS

The authors would like to thank W. Sievers and W. Bröckling for technical assistance. V.D. is grateful to COE at NIRIM, Tsukuba, Japan. O.D. is grateful to the Friedrich-Ebert-Stiftung for financial support.

- ¹J. C. Jamieson, *Science* **139**, 762 (1963).
- ²H. Olijnyk, S. K. Sikka, and W. B. Holzapfel, *Phys. Lett.* **103A**, 137 (1984).
- ³J. Z. Hu and I. L. Spain, *Solid State Commun.* **51**, 263 (1984).
- ⁴Y. K. Vohra, E. Brister, S. Desgreniers, A. L. Ruoff, K. L. Chang, and M. L. Cohen, *Phys. Rev. Lett.* **56**, 1944 (1986).
- ⁵S. J. Duclos, Y. K. Vohra, and A. L. Ruoff, *Phys. Rev. Lett.* **58**, 775 (1987).
- ⁶S. J. Duclos, Y. K. Vohra, and A. L. Ruoff, *Phys. Rev. B* **41**, 12 021 (1990).
- ⁷W. B. Holzapfel, *Rep. Prog. Phys.* **59**, 29 (1996).
- ⁸M. I. McMahon and R. J. Nelmes, *Phys. Rev. B* **47**, 8337 (1993).
- ⁹R. J. Nelmes, H. Liu, S. A. Belmonte, J. S. Loveday, and M. I. McMahon, *Phys. Rev. B* **53**, R2907 (1996).
- ¹⁰M. Hanfland, U. Schwarz, K. Syassen, and K. Takemura, *Phys. Rev. Lett.* **82**, 1197 (1999).
- ¹¹H. Olijnyk and W. B. Holzapfel, *J. Phys. (Paris), Colloq.* **45**, C8-153 (1984).
- ¹²G. V. Raynor and J. A. Lee, *Acta Metall.* **2**, 616 (1954).
- ¹³R. H. Kane, B. C. Giessen, and N. J. Grant, *Acta Metall.* **14**, 605 (1966).
- ¹⁴E. G. Ponyatovskii and V. F. Degtyareva, *High Press. Res.* **1**, 163 (1989).
- ¹⁵V. F. Degtyareva, O. Degtyareva, M. Winzenick, and W. B. Holzapfel, *Phys. Rev. B* **59**, 6058 (1999).
- ¹⁶M. Hansen and K. Anderko, *Constitution of Binary Alloys* (McGraw-Hill, New York, 1958) (reprinted by Genium Publishing Corp., New York, 1989).
- ¹⁷G. C. Che, M. Ellner, and K. Schubert, *J. Mater. Sci.* **26**, 2417 (1991).
- ¹⁸J. W. Otto, *Nucl. Instrum. Methods Phys. Res. A* **384**, 552 (1997).
- ¹⁹K. Takemura and H. Fujihisa, *Phys. Rev. B* **47**, 8465 (1993).
- ²⁰F. Birch, *J. Geophys. Res.* **83**, 1257 (1978).
- ²¹W. B. Holzapfel, *High Press. Res.* **16**, 81 (1998).
- ²²M. Liu and L. Liu, *High Temp.-High Press.* **18**, 79 (1986).
- ²³D. Weaire and A. R. Williams, *Philos. Mag.* **19**, 1105 (1969).
- ²⁴V. F. Degtyareva, M. Winzenick, and W. B. Holzapfel, *Phys. Rev. B* **57**, 4975 (1998).
- ²⁵V. F. Degtyareva, F. Porsch, E. G. Ponyatovskii, and W. B. Holzapfel, *Phys. Rev. B* **53**, 8337 (1996).
- ²⁶V. F. Degtyareva, I. Bdikin, and S. S. Khasanov, *Fiz. Tverd. Tela (St. Petersburg)* **39**, 1509 (1997) [*Phys. Solid State* **39**, 1341 (1997)].